



Hardening behavior of molybdenum by low energy He and D ion irradiation

H. Iwakiri^{a,*}, H. Wakimoto^a, H. Watanabe^b, N. Yoshida^b

^a *Interdisciplinary Graduate School of Engineering Sciences, Kyushu University, Kasuga, Fukuoka 816, Japan*

^b *Research Institute for Applied Mechanics, Kyushu University, Kasuga, Fukuoka 816, Japan*

Abstract

Hardening of Mo by He and D ion irradiation with fusion relevant energy was examined by means of nanoindentation technique and TEM. Steep initial increase of load/displacement–displacement plots and following pop-in movement of the indenter indicate that the subsurface region where the ion-induced damage occurs is hardened. In the early stage of irradiation the hardness increases by about a factor of two due to the formation of dense dislocation loops and saturates for D ion irradiation and He ion irradiation at high temperature. For D ion irradiation, however, one order of higher displacement damage is required to cause similar hardening. In the case of He ion irradiation at 300 K the hardness increases by a factor of four at dose of 1.0×10^{22} ions/m², where a high-density of He bubbles is formed. These results indicate that the irradiation effects of He are much stronger than that of D. © 1998 Elsevier Science B.V. All rights reserved.

1. Introduction

High Z materials such as W and Mo are considered as potential candidates for plasma-facing materials because of their high melting temperature and low sputtering erosion rate. Plasma facing materials suffer exposure of high-density of plasma particles such as H isotopes and He with the energy ranging from some 10 eV to some keV in addition to neutrons. The energetic plasma particles cause not only sputtering but also displacement damage in the subsurface regions where they penetrate directly. It is well known that irradiation of H and He ions at keV energy range causes heavy damage in the directly penetrated region [1]. Experimental techniques for the detection of mechanical property changes in such thin surface layers, however, have been very limited. On the other hand, Shinohara et al., showed that irradiation effects were not limited within the subsurface region of the projected range; irradiation of 100 keV He ion on Mo induced embrittlement at low temperatures and reduced ductility at higher tempera-

tures of thick specimen [2]. In the present work, therefore, effects of fusion relevant low energy He and H ion irradiation on mechanical properties were examined by using a recently developed nanoindentation technique [3], which is suitable for measurement of mechanical properties of thin subsurface regions, and by transmission electron microscopy for complementary observation of microstructure.

2. Experimental procedures

Pure powder metallurgy Mo containing 200, 50, 15, 20 and 5 wppm, respectively, of W, Fe, C, O, and N was rolled to 0.1 mm thick, and cut into disks of 3 mm in diameter. After mechanical polishing and electropolishing they were annealed at 2273 K for 300 s in a vacuum of $<5 \times 10^{-4}$ Pa. Optical microscopy showed that the average grain size was 20 μ m.

Irradiations of He and D ion at 10 keV were carried out in an ultra-high vacuum evacuation apparatus equipped with a small duo-plasmatron type ion gun. The damage range of 10 keV He in Mo was about 80 nm and that of D was about 140 nm. He ion irradiations were performed at 300 and 973 K, respectively, to the dose of

* Corresponding author. Tel.: +81 92 583 7719; fax: +81 92 583 7690; e-mail: iwakiri@he219w.riam.kyushu-u.ac.jp.

about 1×10^{22} He⁺/m². D ion irradiations were carried out at 300 K.

After the irradiations, hardness was measured at room temperature by DUH-50 of Shimadzu Works Ltd., which is a precise load-controlled instrument with a Berkovich-type (trigonal pyramid) diamond tip. The geometry and shape of the indenter have a significant effect on the deformation [4], thus we should use the definition “relative hardness” to evaluate radiation hardening. The indenter load (L) and indenter displacement (d) were continuously monitored by a computer system. Inamura et al., showed that for some metals a L and d relationship of the form,

$$L/d = Ad + B, \quad (1)$$

where A and B are dependent on materials but independent on load and indenter displacement [5,6]. They showed that A is proportional to the Vickers hardness number (H_v) and given by,

$$A(\text{GPa}) = 0.287H_v. \quad (2)$$

Therefore, this analysis is considered to eliminate the elastic effect.

In the present work, therefore, the hardness was estimated by using this relation. Hardness was measured at the central part of the crystal grains to avoid the effects of grain boundaries. Hardness was measured at 20 points for each specimen. Error bars put on each data point in figures in this work show the distribution of the data. Some of the irradiated specimens were annealed at 1173 K for 1 h in a vacuum of 10^{-3} Pa to study the recovery of the radiation effects.

Microstructure of the irradiated specimens was observed by using a JEM-2000EXII electron microscope to correlate of the hardening to the radiation induced defects which may act as obstacles for dislocation movement.

3. Results and discussions

3.1. Irradiation hardening

Typical L/d - d plots for irradiations at 300 K to doses of 1×10^{21} He⁺/m² and 1×10^{22} He⁺/m² are given in Fig. 1(a) together with that of an unirradiated specimen. The projected range of 10 keV He ions and the corresponding damage distribution estimated with TRIM-code are plotted in Fig. 1(b) for comparison. The unirradiated specimen shows good linear relation between L/d and d (see Eq. (1)) through the whole measured range. The hardness of unirradiated specimen estimated by Eq. (2) is about 140. This value agrees well with the standard hardness of annealed Mo. In the irradiated specimens, however, the plots does not show linearity. The gradient of the plot increases with increasing dose at

shallow subsurface region less than about 40 nm in depth, which is about one half of the directly damaged layer. When the displacement distance exceeds about 40 nm the indenter penetrates suddenly and the gradient of the L/d - d plots decreases to the unirradiated level after then.

The sudden penetration described above is similar to so called pop-in phenomenon of hard-coated materials, in which a soft substrate is coated with a hard layer. It is considered that the pop-in phenomenon is connected with the breakthrough of the hard film [7–9]. Chechenin et al. [10] discussed that the pop-in phenomenon occurs when the plastically deformed region formed around indenter tip reaches the film-substrate interface. Based on these studies, the present results can be interpreted as following. The subsurface layer where He ions cause direct damage is hardened and when the plastic zone formed around the indenter tip reaches the interface of the damaged layer and the undamaged substrate, which is likely to about 80 nm in depth, the pop-in occurs. It is reasonable, therefore, to estimate the average hardness of the damage layer from the L/d - d plot before pop-in movement (Fig. 1(a)).

3.2. Dose dependence of radiation hardening

Irradiations with 10 keV-He ions were carried out at 300 and 873 K. The relative hardness and an increase in Vickers hardness, ΔH_v , of the damaged layer estimated from the initial gradient of L/d - d plots are plotted in Fig. 2 as a function of He ion dose. Corresponding displacement damage at the peak depth (25 nm) was also given in the figure. Radiation hardening became appreciable above 8×10^{18} He⁺/m² (0.02 dpa, at the damage peak) for both temperatures. In the case of 873 K-irradiation, relative hardness almost saturates at about 2 above 1×10^{20} He⁺/m² and rather has a tendency to decrease at higher dose around 10^{22} He⁺/m². In the case of 300 K-irradiation, on the other hand, the relative hardness increases with increasing dose however it remains almost constant between 1×10^{20} He⁺/m² and 1×10^{21} He⁺/m². Characteristic feature of the 300 K-irradiation is that the relative hardness increases again above 1×10^{21} He⁺/m² and reaches about 4 at 1×10^{22} He⁺/m² (26 dpa). Such a strong hardening of He ion irradiated Mo at low temperature was also reported by Abe et al. [11].

Fig. 3 shows dose dependence of hardening for 10 keV-D ion irradiation at 300 K. Irradiation hardening also occurs just as He ion irradiation described above but one order of higher displacement damage is required to cause similar hardening. The saturation behaviors are similar for He and D ion irradiations, except for the strong increase above 1×10^{21} He⁺/m² of He ion irradiation at 300 K.

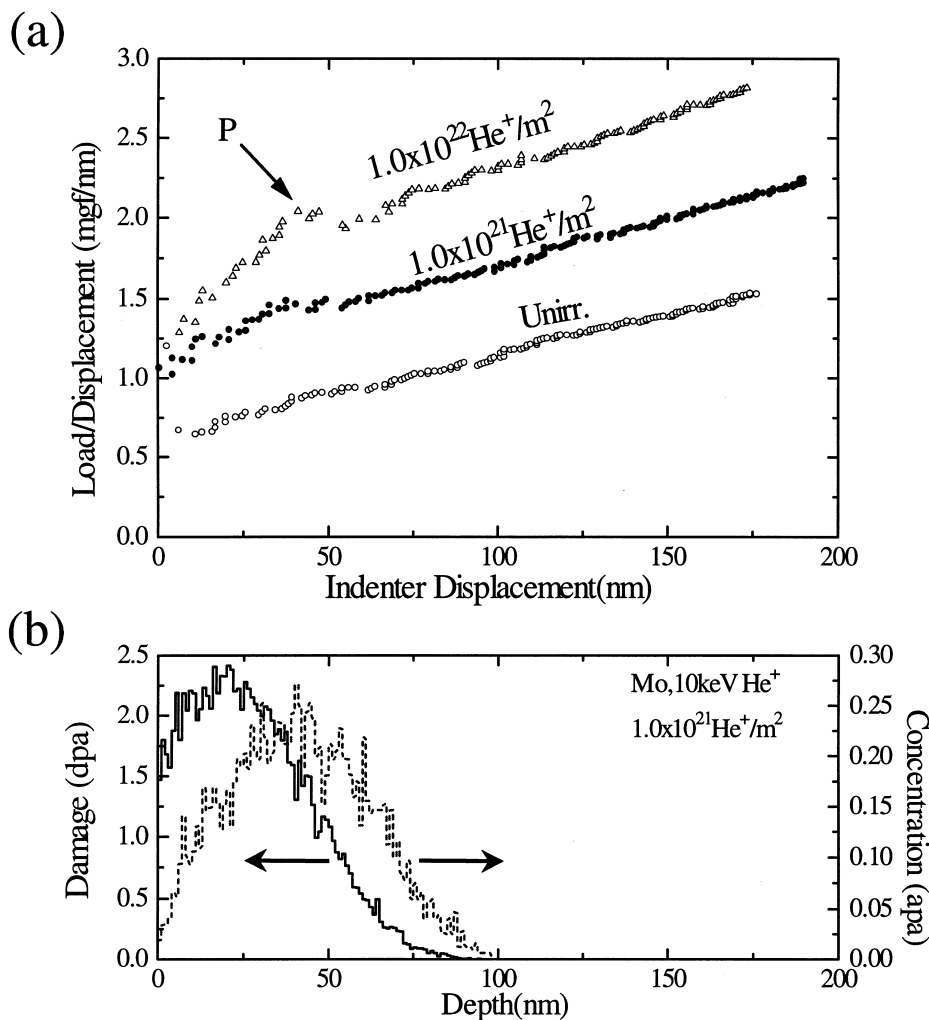


Fig. 1. (a) Typical $L/d-d$ plots for irradiations at 300 K to doses of $1 \times 10^{21} \text{He}^+/\text{m}^2$ and $1 \times 10^{22} \text{He}^+/\text{m}^2$ together with that of un-irradiated specimen. (b) The range and damage distribution calculated with the TRIM code.

3.3. Microstructural evolution and mechanism of irradiation hardening

In order to study the mechanism of irradiation hardening, the radiation induced defects were observed by transmission electron microscopy. Fig. 4 shows the microstructural evolution under 10 keV-He ion irradiation at 300 and 873 K. In both cases interstitial type dislocation loops (black dot images in the photographs) nucleate and grow at first. After the accumulation of a high density of dislocation loops, the nucleation and growth of the loops ceases (Fig. 5). These results lead to the conclusion that interstitial type dislocation loops should be the major origin of irradiation hardening at rather low dose.

In the case of He ion irradiation at 300 K, very dense cavities (white dot images) become visible above 5×10^{20}

He^+/m^2 . It is considered that these dense bubbles contribute to the large hardening above $1 \times 10^{21} \text{He}^+/\text{m}^2$. As shown in Fig. 4, however, the size and density of the bubbles do not change much above $1 \times 10^{21} \text{He}^+/\text{m}^2$ though relative hardness increases from 1.8 to 3.9. A possible explanation of the hardening is the following. Most of the injected He atoms are trapped in pre-existing bubbles and increase their inner pressure to very high values [12,13]. It is likely that the high-pressure bubbles induce stress in the surrounding materials and cause hardening.

In the case of He ion irradiation at 873 K, bubbles are also formed above $5 \times 10^{20} \text{He}^+/\text{m}^2$. As one can see in Fig. 4, the dense bubbles increase their size by coarsening. For example, by increasing the dose from $10^{21} \text{He}^+/\text{m}^2$ to $10^{22} \text{He}^+/\text{m}^2$ the average size becomes about five times larger but the density decrease more

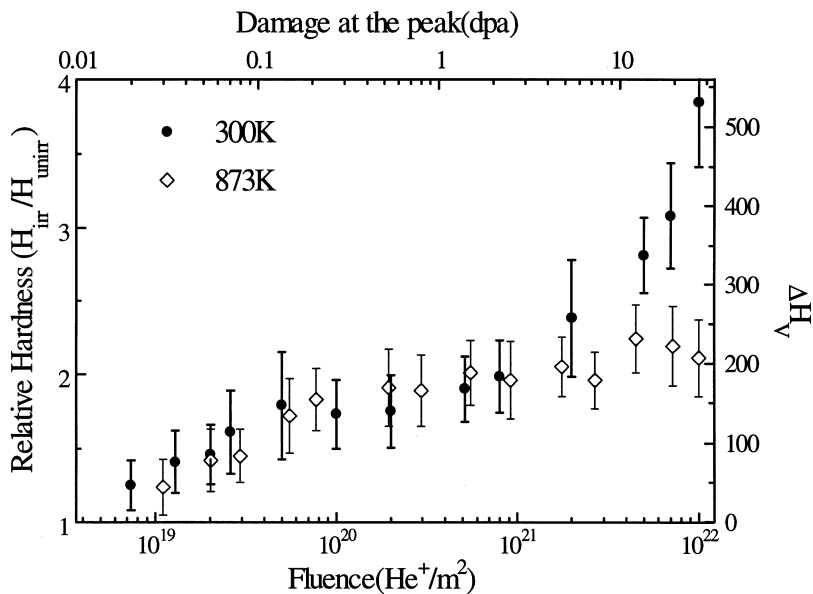


Fig. 2. Dose dependence of the hardening of the damaged layer for 10 keV-He ion irradiation at 300 and 873 K.

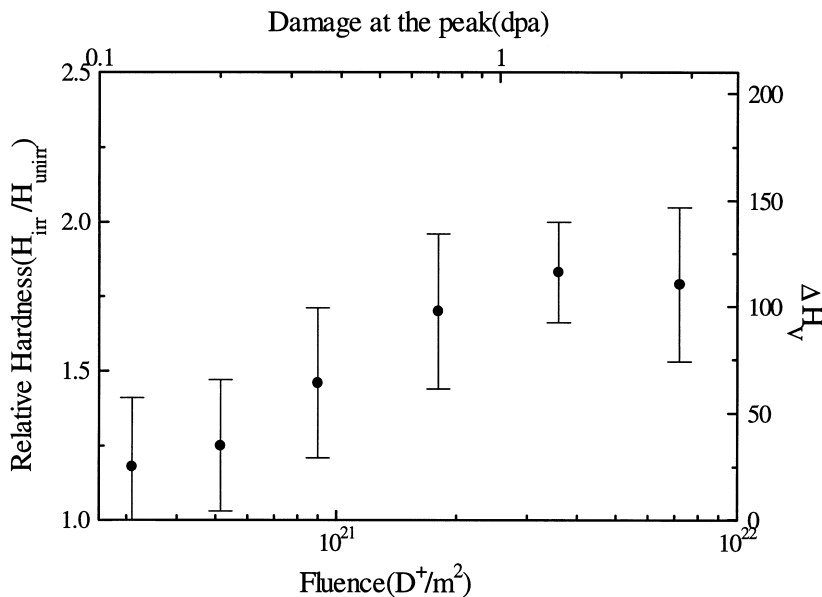


Fig. 3. Dose dependence of the hardening of the damaged layer for 10 keV-D ion irradiation at 300 K.

than one order of magnitude. One should note that the shape of the bubbles is not roundish at $1 \times 10^{22} \text{ He}^+/\text{m}^2$. This implies that the pressure of He gas in these bubbles is rather low. It seems that the hardness does not increase much above $1 \times 10^{21} \text{ He}^+/\text{m}^2$ in spite of the coarsening, because of the reduction of dislocation density.

Fig. 5 shows the microstructural evolution under 10 keV-D ion irradiation at 300 K. Only a small number of loops are seen at $2.5 \times 10^{20} \text{ ions}/\text{m}^2$ (0.1 dpa, at the damage peak), and the density and size of loops increase at $1.0 \times 10^{21} \text{ ions}/\text{m}^2$. No significant change in microstructure was observed in further irradiation. The dislocation loop nucleation rate of D ion irradiated

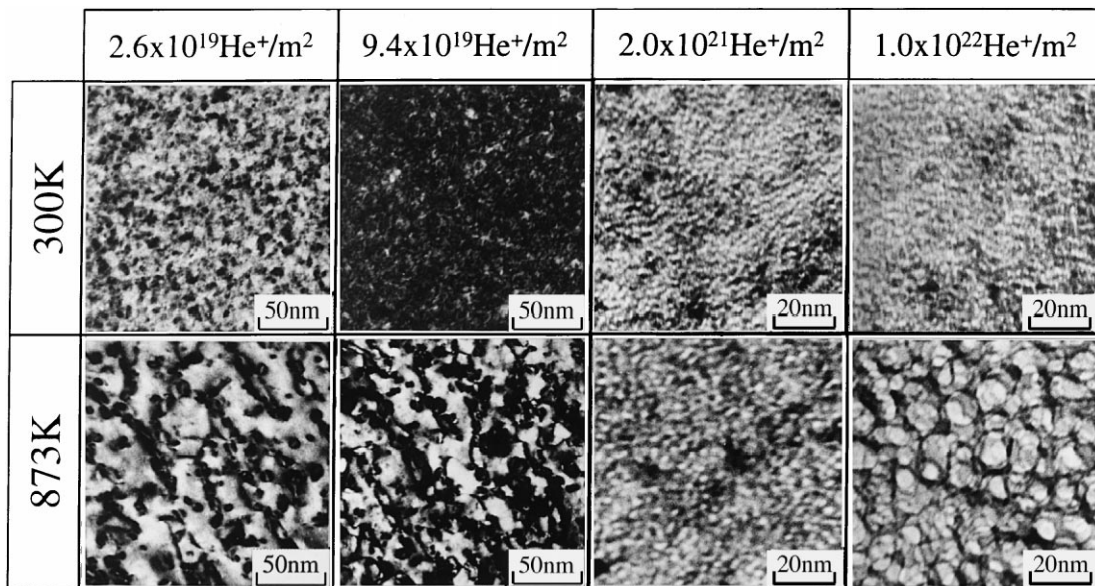


Fig. 4. Microstructural evolution of Mo at 300 and 873 K during irradiation with 10 keV-He ion.

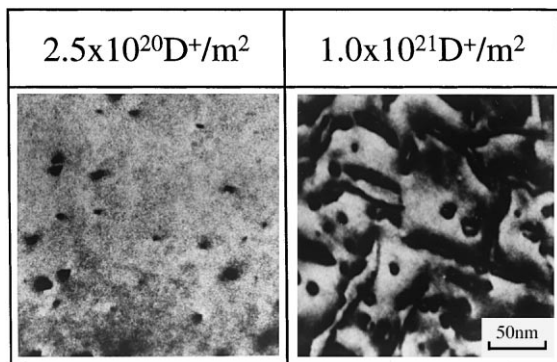


Fig. 5. Microstructural evolution of molybdenum at 300 K during irradiation with 10 keV-D ion.

specimen is more than one order of magnitude lower. These results indicate that the nucleation mechanism of interstitial loops in He ion irradiation and D ion irradiation is different. Details of the mechanism will be discussed in elsewhere. Niwase et al. have also found that the effect of implanted He on the loop formation in Ni is much stronger than that of implanted D [14].

The recovery of irradiation induced hardening was also examined. Fig. 6 shows changes of relative hardness for He and D ion irradiations at 300 K, respectively, by the annealing at 1173 K for 1 h. For D ion irradiation, hardening almost recovered after the annealing, while it remains considerably for He ion irradiations. The dislocation loops formed in W by He ion irradiation did

not change even by annealing at 1373 K [15], at which temperature those by H ion irradiation were annihilated completely. It may be assumed that He atoms increase thermal stability of dislocation loops and thus hardening remains even after the annealing. We need more experiments to understand the details of the annealing effects on hardening but a possible explanation for the reduction of hardening of He ion irradiation to $1 \times 10^{22} \text{He}^+/\text{m}^2$ is the reduction of gas pressure of over-pressured bubbles by annealing.

4. Summary

Hardening of Mo by the irradiation with He and D ions in the fusion relevant keV range energy was examined by means of nanoindentation technique and TEM. Steep initial increase of $L/d-d$ plots and following pop-in movement of the indenter tip indicate that the subsurface region where irradiation damage occurs directly by the bombarded ions caused hardening. In the case of irradiation with He and D ions at 300 K, radiation induced dislocations (loops) cause hardening at first. The relative hardness normalized by the unirradiated value reaches about 2. The relative hardness of He ion irradiated specimen reaches about 4 by high dose, where a dense structure of small He bubbles is formed. It seems that the formation of high-pressured bubbles results in strong hardening. Due to the formation of radiation induced defects such as dislocations (loops) and large cavities, relative hardness of the subsurface region reaches to about 2 even at 873 K.

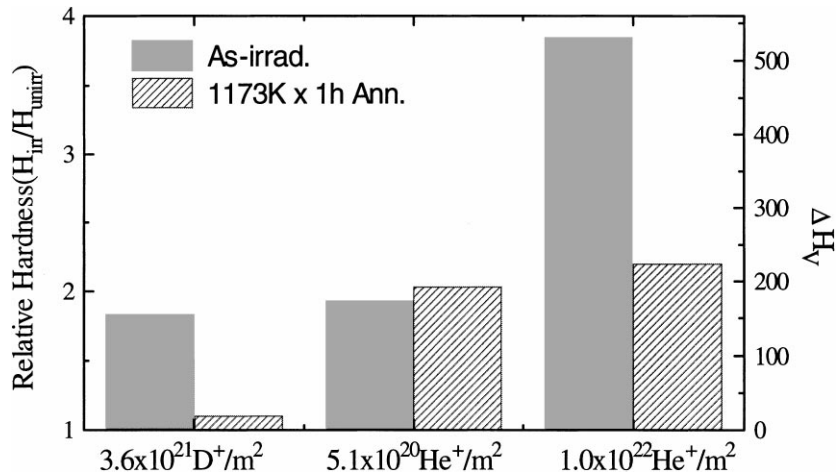


Fig. 6. Changes of hardening for 10 keV-He ion and D ion irradiations at 300 K by the annealing at 1173 K for 1 h.

Present results indicate that the plasma facing materials, especially metallic ones, in D-T burning devices suffer radiation hardening by the bombardment of He particles from the plasma. It should be emphasized that this degradation of mechanical properties by He particles is one of the key issues for high Z plasma facing materials.

References

- [1] R. Sakamoto, T. Muroga, N. Yoshida, *J. Nucl. Mater.* 212–215 (1994) 1426.
- [2] K. Shinohara, A. Kawakami, S. Kitajima, Y. Nakamura, M. Kutsuwada, *J. Nucl. Mater.* 179–181 (1991) 246.
- [3] J.B. Pethica, R. Hutchings, W.C. Oliver, *Philos. Mag. A.* 48 (1982) 593.
- [4] C.W. Shih, M. Yang, J.C.M. Li, *J. Mater. Res.* 6 (1991) 2623.
- [5] M. Inamura, T. Suzuki, *Seisan Kenkyu.* 42 (1990) 257.
- [6] J. Ohta, T. Ohmura, K. Kako, M. Tokiwai, T. Suzuki, *J. Nucl. Mater.* 225 (1995) 187.
- [7] A.J. Whitehead, T.F. Page, *Thin Solid Films* 220 (1992) 277.
- [8] J.C. Knight, A.J. Whitehead, T.F. Page, *J. Mater. Sci.* 27 (1992) 3939.
- [9] T.F. Page, S.V. Hainsworth, *Surf. Coat. Technol.* 61 (1993) 201.
- [10] N.G. Chechenin, J. Böttiger, J.P. Korg, *Thin Solid Films* 261 (1995) 228.
- [11] K. Abe, A. Hasegawa, M. Kikuchi, S. Morozumi, *J. Nucl. Mater.* 103&104 (1981) 1169.
- [12] W.G. Wolfer, *J. Nucl. Mater.* 93&94 (1980) 713.
- [13] W. Jäger, R. Manzke, H. Trinkaus, G. Grecelius, R. Zeller, *J. Nucl. Mater.* 111&112 (1982) 674.
- [14] K. Niwase, T. Ezawa, T. Tanabe, M. Kiritani, F.E. Fujita, *J. Nucl. Mater.* 203 (1993) 56.
- [15] H. Iwakiri, N. Yoshida, unpublished.